*Articles*

# Distributions of Proteins and Lipids in the Erythrocyte Membrane†

William Rodgers and Michael Glaser*

*Department of Biochemistry, University of Illinois, Urbana, Illinois 61801*

*Received June 16, 1993; Revised Manuscript Received August 24, 1993®*

ABSTRACT: Fluorescence digital imaging microscopy was used to characterize erythrocyte membrane domains. To investigate the role of specific proteins in forming lipid domains, erythrocyte ghosts were double-labeled with fluorescent phospholipids and a fluorescent label specific for band 3, the major integral membrane protein. Areas of enrichment, or domains, were observed for both the protein and lipid components. The size and enrichment of the protein and lipid domains in the membrane depended upon the ionic strength but not the temperature. Also, there was a higher correlation between the areas of band 3 and phosphatidylcholine enrichment than between band 3 and phosphatidylserine enrichment. This is consistent with band 3 playing a role in the formation of the phosphatidylcholine domains. Furthermore, areas of spectrin enrichment also were observed in immunofluorescently labeled ghosts, and the band 3 domains were found to coincide with the spectrin domains. Thus, the distribution of band 3 in ghosts is influenced by interactions with the cytoskeleton. Together, these experiments illustrate the type of membrane heterogeneity present in erythrocyte ghosts and the type of lipid and protein interactions that can affect the domains.

Biological membranes consist of an assortment of protein and lipid components, and they represent the site of a large number of cellular processes such as transmembrane signaling (Hollenberg, 1991), protein translocation and sorting (Singer, 1990; Pfeffer & Rothman, 1987), and cell–cell recognition (McClay & Ettensohn, 1990). The topology, or the lateral distribution of the proteins and lipids in the membrane, may play an important role in the mechanism of these processes. There is substantial evidence for lateral heterogeneity in biological membranes, with the membrane proteins and lipids being enriched into domains (Pessin & Glaser, 1980; Shukla & Hanahan, 1982; Jain, 1983; Gordon & Mobley, 1984; Thompson & Tillack, 1985; Metcalf *et al.*, 1986; Haverstick & Glaser, 1987; Finzi *et al.*, 1989; Wolf *et al.*, 1990; Tocanne *et al.*, 1989; Yechial & Edidin, 1987; Kinnunen, 1991; Rodgers & Glaser, 1991, 1993; Edidin & Stroynowski, 1991; Edidin *et al.*, 1991; Glaser, 1993). These domains represent areas in the membrane where the concentrations of proteins and lipids are different from the bulk membrane.

A variety of mechanisms may be responsible for forming membrane domains. In human erythrocytes, the major cytoskeletal protein spectrin is anchored to the membrane by binding to the anion transporter protein band 3 via ankyrin and also to glycophorin via band 4.1 (Bennett, 1985). Band 3 has a subunit molecular weight of 89 000, and it is the most abundant integral membrane protein. When band 3 interacts with the cytoskeletal matrix its lateral mobility is restricted (Fowler & Branton, 1977; Jacobson *et al.*, 1987; Golan & Veatch, 1980; Sheetz *et al.*, 1980). Membrane protein anchoring to the cell cytoskeleton may provide a means for forming and stabilizing membrane domains. Membrane protein anchoring to the cell cytoskeleton has been used to explain protein enrichment in such cases as polarized epithelial cells, receptor clustering at nerve terminals, and domains of the MHC molecules H-2D$^b$ (Morrow, 1989; Phillips *et al.*, 1991; Edidin & Stroynowski, 1991; Edidin *et al.*, 1991). As in erythrocyte membranes, the cytoskeleton is ascribed the role of limiting the free lateral diffusion of the membrane proteins and thereby inducing their enrichment in specific areas of the cell membrane.

Specific protein–lipid interactions may provide another mechanism for formation and stabilization of membrane domains. In such cases, enrichment of membrane lipids could occur by interacting with specific proteins that either bind or are inserted into the membrane. Specific examples of this include enrichment of acidic phospholipids by cytochrome *c* and protein kinase C (Haverstick & Glaser, 1989; Bazzi & Nelsestuen, 1991). Spectrin also is known to bind to phospholipids with low affinity, particularly phosphatidylserine (Haest, 1982). Other examples that may be important for the formation of domains include cases where membrane protein self-association was found to depend on the lipid composition of the membrane (Rothberg *et al.*, 1990; Muhlebach & Cherry, 1982).

The use of fluorescence digital imaging microscopy (FDIM)[1] to study lipid domains in erythrocyte membranes has been described (Haverstick & Glaser, 1987; Rodgers & Glaser, 1991, 1993). In these experiments, FDIM proved to be a versatile technique that provided detailed information about the lateral heterogeneity of the erythrocyte membrane. The

† This work was supported in part by a grant from the American Cancer Society (BE-167). W.R. was the recipient of a Kodak Fellowship.

* Author to whom correspondence should be addressed: Department of Biochemistry, University of Illinois, 600 S. Mathews Ave., Urbana, IL 61801 (Phone, 217-333-3960; Fax, 217-244-5858).

® Abstract published in *Advance ACS Abstracts,* November 1, 1993.

[1] Abbreviations: dansyl-PC, 1-acyl-2-[4-[*N*-[5-(dimethylamino)naphthalene-1-sulfonyl]amino]butanoyl]phosphatidylcholine; dansyl, 1-acyl-2-[4-[*N*-[5-(dimethylamino)naphthalene-1-sulfonyl]amino]butanoyl]; FDIM, fluorescence digital imaging microscopy; NBD, 1-acyl-2-[[*N*-(4-nitrobenz-2-oxa-1,3-diazolyl)amino]caproyl]; NBD-PC, 1-acyl-2-[[*N*-(4-nitrobenz-2-oxa-1,3-diazolyl)amino]caproyl]phosphatidylcholine; NBD-PS, 1-acyl-2-[[*N*-(4-nitrobenz-2-oxa-1,3-diazolyl)amino]caproyl]phosphatidylserine; PBS, 137 mM NaCl, 3 mM KCl, 6 mM $Na_2HPO_4$, and 2 mM $KH_2PO_4$, pH 7.4; SITS, 4-acetamido-4′-isothiocyanatostilbene-2,2′-disulfonic acid.

0006-2960/93/0432-12591$04.00/0 

results of these studies also suggested that membrane proteins are important in forming the lipid domains. In order to determine the role of specific proteins in forming lipid domains, this paper reports FDIM experiments on two major erythrocyte membrane associated proteins, band 3 and spectrin. The topology of these proteins in relation to lipid domains was investigated using a combination of double-labeling experiments with either a fluorescent label specific for band 3, immunofluorescence staining for spectrin, or fluorescent phospholipids.

## MATERIALS AND METHODS

*Ghost Preparation.* Rabbit erythrocytes were collected and stored as described previously (Rodgers & Glaser, 1991). The ghosts were prepared by the method of Lee *et al.* (1985) using a 5.0 mM sodium phosphate buffer (pH 7.4) for lysis. After lysis and centrifugation in a microfuge (17000*g*, 2 min) the ghosts were washed, usually two to three times, until the supernatant was free of hemoglobin. After the final wash, the ghosts were suspended in 5.0 mM phosphate buffer to a volume 10-fold larger than the volume of the membrane pellet.

*Fluorescence Labeling.* Specific labeling of band 3 was done using 4-acetamido-4′-isothiocyanatostilbene-2,2′-disulfonic acid (SITS, U.S. Biochemicals). Intact erythrocytes were washed two to three times and resuspended in a 5-fold volume of 137 mM NaCl, 3 mM KCl, 6 mM $Na_2HPO_4$, and 2 mM $KH_2PO_4$, pH 7.4 (PBS). The final resuspension was done in PBS containing 1.0 mM SITS (Knauf & Rothstein, 1971). The cells were stirred in the dark at room temperature for 30–45 min and then washed several times with PBS. The cells were lysed as described above. Sodium dodecyl sulfate–polyacrylamide gel electrophoresis of SITS-labeled membranes followed by UV transillumination revealed band 3 to be the only fluorescently labeled protein.

Unsealed ghosts were labeled with the fluorescent phospholipid 1-acyl-2-[[*N*-(4-nitrobenz-2-oxa-1,3-diazolyl)amino]-caproyl]phosphatidylcholine (NBD-PC) or 1-acyl-2-[[*N*-(4-nitrobenz-2-oxa-1,3-diazolyl)amino]caproyl]phosphatidylserine (NBD-PS) using donor vesicles as described previously (Rodgers & Glaser, 1991). NBD-PS was synthesized from NBD-PC as described by Haverstick and Glaser (1987). Donor vesicles containing 0.2–0.4 nM total lipid were added per 100 μL of ghost suspension and incubated at 4 °C for 20 min. The ghosts were washed twice with 5 mM phosphate buffer and suspended in either 5 mM phosphate buffer or PBS. The ghosts in PBS were washed one additional time with PBS. All washes were done at 4 °C.

For the immunofluorescence labeling of spectrin, unsealed ghosts in 5 mM phosphate buffer were incubated for 1 h with an anti-spectrin (α and β) monoclonal antibody (mouse IgM in ascites fluid; Sigma Chemical Co.). The ghosts were washed several times and resuspended in 5 mM phosphate buffer, followed by another 1-h incubation with fluorescein-conjugated anti-mouse IgM antibody (Sigma Chemical Co.). The ghosts were washed several times and resuspended in either 5 mM phosphate buffer or PBS for microscopy. All incubations and washes were done at 4 °C. For the ghosts suspended in PBS, the sample was washed with PBS prior to the final resuspension. To check for cross-reactivity, ghosts were incubated with normal mouse ascites fluid, followed by the secondary antibody. Microscopy of these control ghosts revealed no immunofluorescence staining.

*Fixation.* Unsealed ghosts were fixed using a 0.5% solution of glutaraldehyde in PBS as described by Daleke and Huestis (1985). Prior to fixing, the ghosts were washed and suspended in PBS, and 500 μL of the ghost suspension was added to 5.0 mL of the glutaraldehyde solution, followed by stirring for 30 min. The ghosts were washed several times and suspended in PBS, followed by immunofluorescence labeling of spectrin as described above.

*Fluorescence Microscopy.* All fluorescence microscopy was done using the system previously described (Rodgers & Glaser, 1991). For NBD and fluorescein imaging, excitation was between 420 and 460 nm. For dansyl and SITS imaging, excitation was between 340 and 380 nm. Emission wavelengths greater than 430 nm were collected for dansyl and SITS imaging, and wavelengths greater than 515 nm were collected for NBD and fluorescein imaging. A thermoregulated microscope stage was used to control the temperature (Leitz heating and cooling stage 80). The samples were allowed to equilibrate for 2 min on the stage before collection of the image. The thermoregulated stage was maintained at the desired temperature ±2 °C.

*Image Processing and Quantitation.* Background subtraction and normalization of the images were done with the final images having a mean gray value of 100 ± 4 on a gray scale of 0–255 (Figure 1, bottom) (Rodgers & Glaser, 1991). The area used for the normalization operations was a square enclosing the edge of the ghost. Identical areas were used in normalizing the companion images of double-labeled ghosts.

The radiance values of the domains were measured using the pixel with the greatest or the smallest gray value in the areas of enrichment or depletion, respectively. The domains were visually defined using the pseudo-color assignment of pixel radiance. Since most of the pixels in the normalized images are green, the domains were assigned to the colors above and below the green on the pseudo-color scale (Figure 1, bottom). Quantitatively, this typically corresponded to radiance values above 155 for the areas of enrichment and less than 100 for the areas of depletion. For construction of the surface plots, the pixel in the corresponding position in the companion image was also measured. This generated two radiance values for each area of enrichment or depletion. The same domain was measured twice in each companion image when both fluorophores were enriched, but the maximum radiance values did not coincide. This also applies to the areas of depletion for the minimum radiance values.

Measurements of the areas of enrichment in normalized images were done by first subtracting 135 from each pixel gray value in the image to define the boundary of the enriched area. Subtraction of 135 ensures that all the pixels associated with each area of enrichment were included in the measurements. The resulting pixel gray values were multiplied by six. This produced a sharply defined border around the region or enrichment. The domains of enrichment were outlined and the area inside the outlines measured using an area function. The area measurements for the depleted regions were done as described for the areas of enrichment. However, the gray scale was first inverted so that a radiance of 255 equaled 0.

## RESULTS

*Effects of Ionic Strength and Temperature on Membrane Domains.* Previous studies have suggested that proteins are responsible for forming lipid domains in the erythrocyte membrane (Rodgers & Glaser, 1991, 1993). To characterize the distribution of a specific protein in the membrane, the major erythrocyte glycoprotein band 3 was labeled using the fluorescent affinity label 4-acetamido-4′-isothiocyanatostilbene-2,2′-disulfonic acid (SITS). The ghosts were further

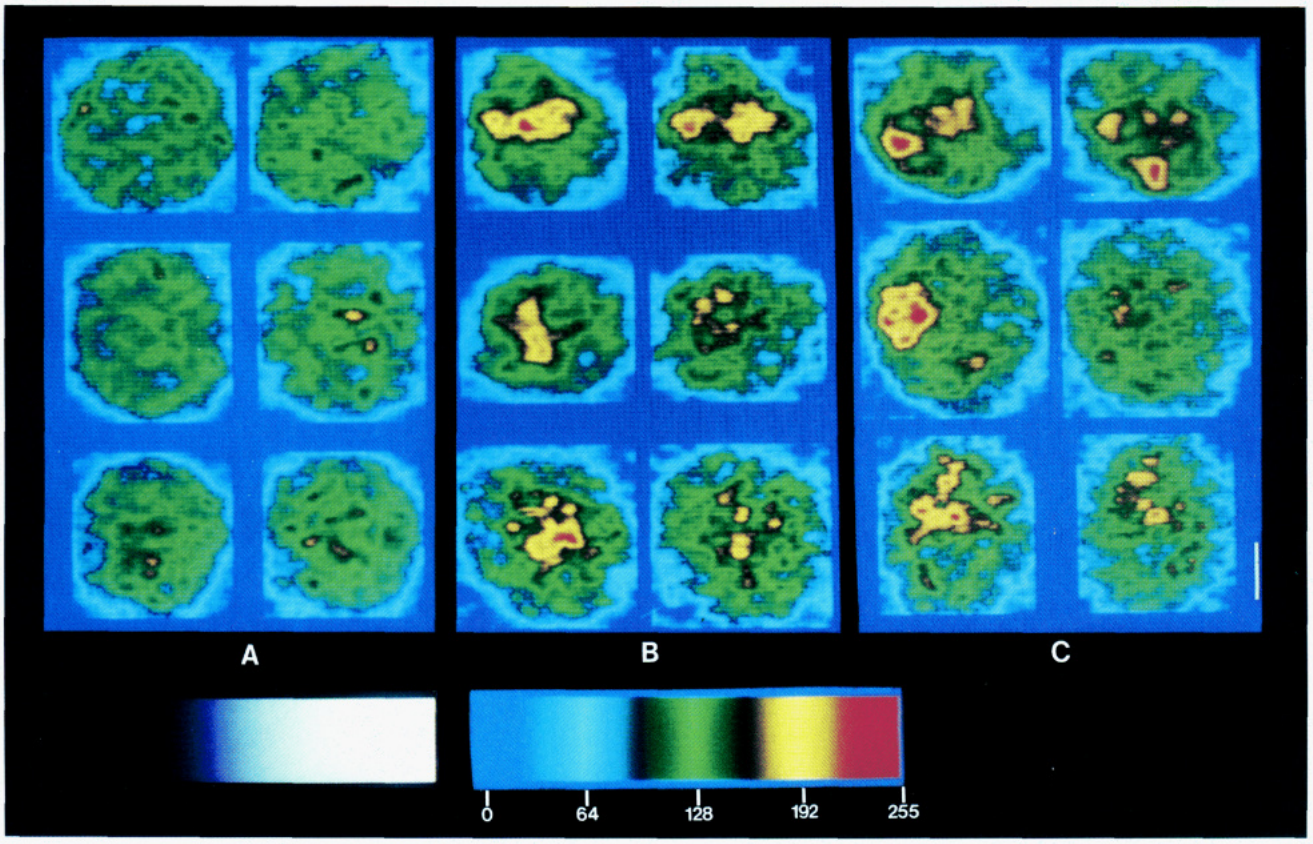


FIGURE 1: Erythrocyte ghosts double-labeled with NBD-PC and SITS-labeled band 3. Three different ghosts are shown in each panel, and each panel represents ghosts in either 5 mM phosphate buffer at 4 °C (A), PBS at 4 °C (B), or PBS at 37 °C (C). The NBD-PC images are on the left, and the SITS images are on the right for each ghost. All images were normalized to a mean gray value of 100 ± 4. The white bar equals 2.5 μm. The pseudo-color scheme applied to the images is shown with its equivalent gray values (bottom). The gray values range from 0 (blue) to 255 (red). The two grey bands in the pseudo-color scale result from color mixing by the television monitor from which the images are photographed.

labeled with NBD-labeled phospholipids to correlate the distribution of band 3 and phospholipids in the membrane.

Band 3 has several advantages that make it well suited for FDIM. These include its high copy number in the membrane (Bennett, 1985) and the information that is available on the lateral and rotational mobility of band 3 (Golan & Veatch, 1980; Matayoshi & Jovin, 1991; Tsuji *et al.*, 1988). These studies showed that band 3 can exist as a dimer, a tetramer, and higher oligomers. Of particular interest for the present study was the observation that the immobile fraction of band 3 increased at higher ionic strengths (Golan & Veatch, 1980). The effects of ionic strength and temperature on the distributions of band 3 and different phospholipids were determined in ghosts suspended in either 5 mM phosphate buffer (Figure 1A), PBS at 4 °C (Figure 1B), or PBS at 37 °C (Figure 1C). The NBD-PC images are on the left and the SITS-labeled band 3 images are on the right.

It is evident in Figure 1 that the distributions of both band 3 and phosphatidylcholine were not uniform in all the conditions studied. For example, in each ghost the distributions of band 3 and phosphatidylcholine had a unique pattern of enrichment and depletion in the membrane. When the ghosts were suspended in the low ionic strength buffer (5 mM phosphate buffer), the domains were smaller and less enriched compared with the domains in the ghosts suspended in PBS. Furthermore, the ghosts in PBS at 4 and 37 °C showed similar types of large, intense domains relative to the less enriched, smaller domains present in ghosts in 5 mM phosphate buffer. The distributions of band 3 and phosphatidylcholine were, therefore, significantly affected by the ionic strength but not the temperature of the sample. Also there was a correlation between the enrichment of band 3 and NBD-PC, which is consistent with the suggestion that interactions between membrane proteins and lipids are important in forming the domains. If the domains were due to a lipid phase transition and the coexistence of gel and liquid–crystalline lipids, a strong temperature dependence would be expected. In addition, no evidence for a lipid phase transition was obtained in vesicles composed of extracted erythrocyte lipids. No changes in the lipid distribution occurred as a function of either ionic strength or temperature (data not shown).

To characterize the phosphatidylcholine and band 3 distributions in a population of ghosts, images of 50–60 ghosts were collected. The radiance values of the phosphatidylcholine and band 3 domains were measured in both the areas of enrichment and depletion, and the results are shown in the surface plots in Figure 2. In these plots, each axis represents the radiance value of the pixel in either the NBD-PC image ($x$-axis) or the SITS image ($y$-axis). The height at each point ($z$-axis) represents the frequency of the domains with the corresponding NBD-PC and SITS pixel radiance values. An imaginary diagonal passing from the origin across the surface of the $x$-$y$ plane represents the pixels where the SITS and the NBD-PC radiance values were equal. Ghosts double-labeled with NBD-PC and dansyl-PC had their domain radiance values distributed entirely along this diagonal (Rodgers & Glaser, 1993). Conversely, areas of the plots away from the diagonal represent domains with unequal enrichment or depletion of SITS and NBD-PC. The empty space in the middle of the plots represents radiance values that were not associated with domains.

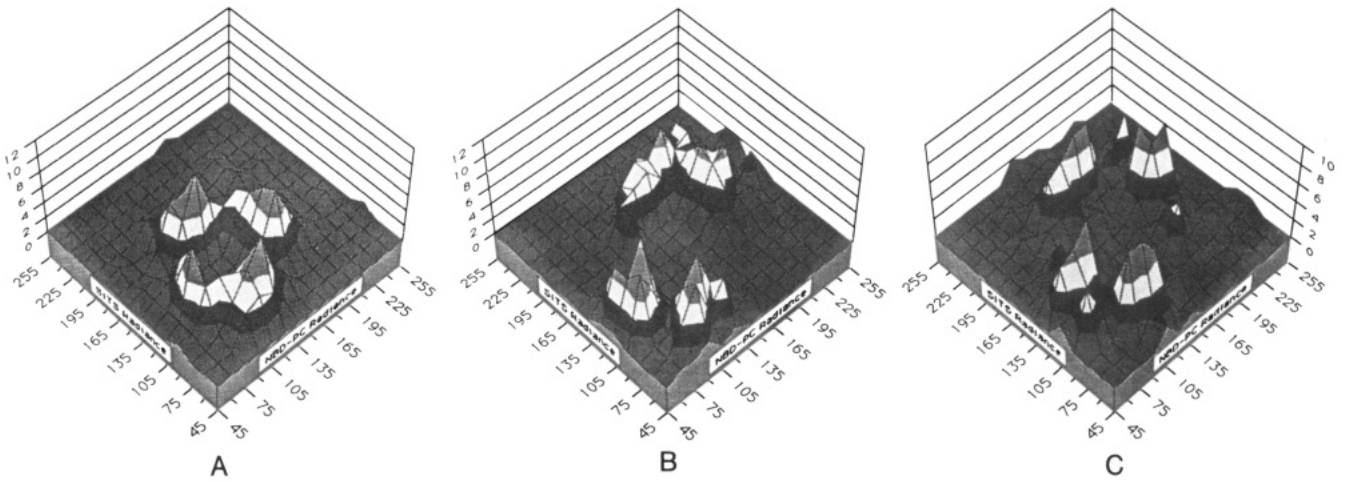


FIGURE 2: Surface plots showing the distributions of domain radiance values for a population of ghosts double-labeled with NBD-PC and SITS-labeled band 3 as in Figure 1. The surface plots show the number of domains ($z$-axis) with the corresponding NBD-PC ($x$-axis) and SITS ($y$-axis) radiance values. The ghosts were in either 5 mM phosphate buffer at 4 °C (A), PBS at 4 °C (B), or PBS at 37 °C (C), with population sizes of 52, 69, and 58, respectively. The images are normalized to a mean gray value of 100 ± 4 prior to measurement.

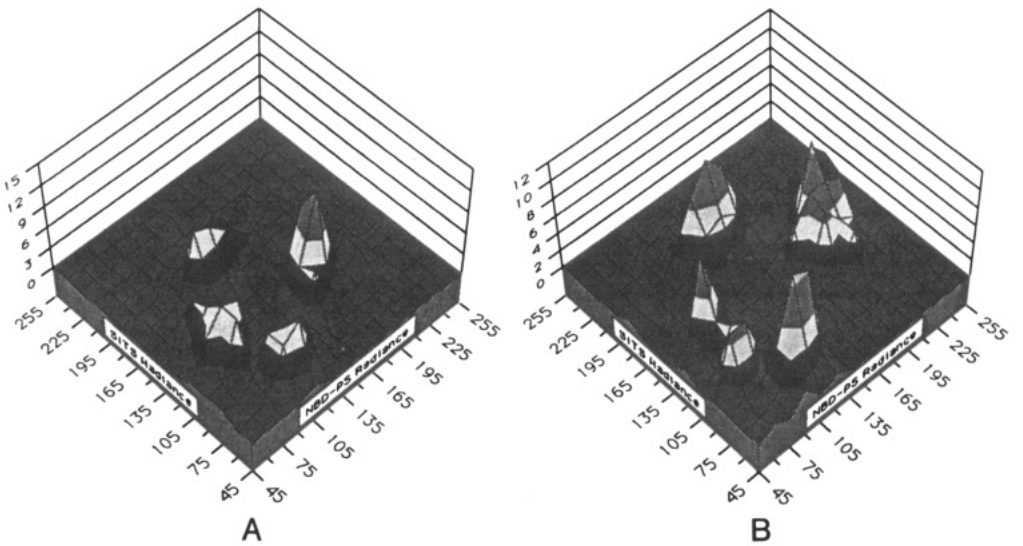


FIGURE 3: Surface plots showing the distributions of domain radiance values for a population of ghosts double-labeled with NBD-PS and SITS-labeled band 3. The surface plots were constructed as described in Figure 2. The ghosts were suspended in either 5 mM phosphate buffer at 4 °C (A) or PBS at 4 °C (B). The sizes of the ghost populations used for the measurements were 34 and 38 for the samples in 5 mM phosphate buffer and PBS, respectively.

The changes in the domain enrichment that are visible in Figure 1A,B for individual ghosts suspended in PBS rather than 5 mM phosphate buffer are also evident in the surface plots presented in Figure 2 for the population of ghosts. For example, the distribution of radiance values shifts along the $x$-$y$ diagonal to include greater enrichment in the band 3 and phosphatidylcholine domains in ghosts suspended in PBS at 4 °C relative to the domains in the ghosts in 5 mM phosphate buffer (Figure 2, panel B versus panel A). The shift in the distribution along the $x$–$y$ diagonal also suggests that band 3 may be important in forming the phosphatidylcholine domains. In cases where there is no interaction between two components, greater enrichment of one component would occur independently of the second component. This would shift the distribution in the $x$ or $y$ direction only, rather than along the $x$–$y$ diagonal. Changes of this nature occur when $Ca^{2+}$ is added to ghosts and there is an enrichment of phosphatidylserine without a comparable increase in phosphatidylcholine (Rodgers & Glaser, 1993). Figure 2 also shows the distribution of domain radiance values for ghosts in PBS at 37 °C (Figure 2C). The peaks in this plot appear slightly sharper compared with ghosts in PBS at 4 °C. However, the ranges of domain radiance values are similar at both temperatures.

The possibility that band 3 may exhibit some specificity in forming phosphatidylcholine domains was addressed by double-labeling ghosts with SITS and NBD-PS. Some of the observations that were made concerning domains in ghosts double-labeled with SITS and NBD-PC also applied to the ghosts double-labeled with SITS and NBD-PS. For example, Figure 3 shows the distributions of domain radiance values for separate populations of ghosts double-labeled with NBD-PS and SITS and suspended in either 5 mM phosphate buffer (Figure 3A) or PBS (Figure 3B) at 4 °C. The increase in the domain enrichment for ghosts in PBS compared with ghosts in 5 mM phosphate buffer is evident by the shift in the distributions to greater radiance values. The images of the ghosts represented in Figure 3 also had a heterogeneous distribution of both band 3 and phosphatidylserine, with each image having its own unqiue pattern of enrichment and depletion.

The surface plots in Figure 3 show a smaller correlation between band 3 and NBD-PS in the domains compared with band 3 and NBD-PC in the domains shown in Figure 2. The domain radiance distributions for band 3 and NBD-PS are

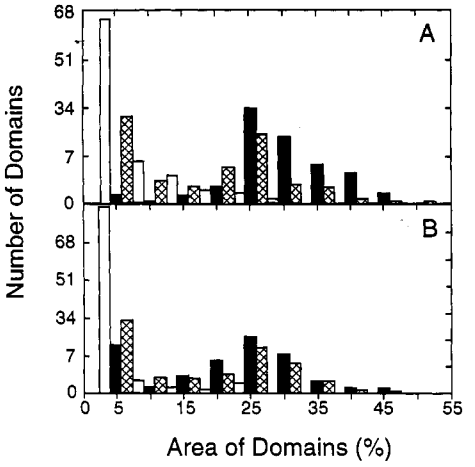


FIGURE 4: Distributions of the relative areas of enrichment for double-labeled ghosts. The distributions are for the relative areas of enrichment in the NBD-PC (A) and SITS-labeled band 3 (B) images of ghosts in either 5 mM phosphate buffer at 4 °C (□), PBS at 4 °C (■), or PBS at 37 °C (crosshatched □). The area of the domain represents the percent of the area of the total image. The areas were measured in the same ghosts that generated the data for Figure 2. The images were normalized to a mean gray value of 100 ± 4 prior to measurements. Domain areas that were less than 1% of the entire area of the image were not included in the distribution.

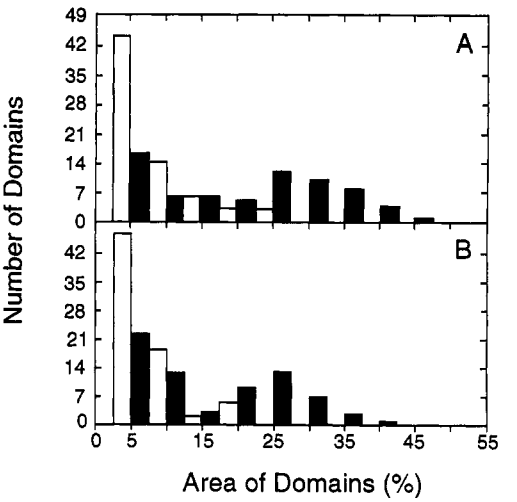


FIGURE 5: Distributions of domain sizes for ghosts double-labeled with NBD-PS and SITS-labeled band 3. The distributions are for the areas of enrichment in the NBD-PS (A) and SITS (B) images of ghosts in either 5 mM phosphate buffer at 4 °C (□) or PBS at 4 °C (■). The areas were measured in the same ghosts that generated the data for Figure 4. The images were normalized to a mean gray value of 100 ± 4 prior to measurement. Domain areas that were less than 1% of the entire area of the image were not included.

shifted away from the $x$–$y$ diagonal relative to the distributions for band 3 and NBD-PC in corresponding conditions (Figure 3 versus Figure 2). Thus, there is a lower concentration of NBD-PS than NBD-PC in the areas of band 3 enrichment.

The maximum range of concentration of each fluorophore in the ghosts from Figures 2 and 3 was measured by taking the ratio of the largest over the smallest radiance value in each image. In cases where the radiance value in the normalized image was at the saturated value of 255, the values were measured in the prenormalized image. The maximum concentration ranges for the different fluorophores in each population of ghosts averaged between 2.0 and 3.5, with the ghosts in PBS usually having an average value greater than 3.0. The largest range of concentrations measured for the entire sample of images represented in Figures 2 and 3 were 6.8, 4.0, and 8.5 for NBD-PC, NBD-PS, and SITS, respectively, for ghosts suspended in PBS.

It is also apparent in Figure 1 that the domains increased in size when the ghosts were suspended in PBS rather than 5 mM phosphate buffer. The distributions of the domain areas for the ghosts in the separate conditions are shown in Figure 4 for the NBD-PC (top) and the SITS images (bottom). The majority of the domains for ghosts in 5 mM phosphate buffer had areas less than 5% of the image. When the ghosts were shifted to PBS, at either 4 or 37 °C, there was a decrease in the number of small domains and an increase in domains with areas between 20% and 30% of the image. This resulted in a bimodal distribution for the SITS domains of ghosts in PBS at 4 °C and in the distributions for both the SITS and the NBD-PC domains in ghosts in PBS at 37 °C.

Figure 5 shows the distributions of domain sizes for ghosts double-labeled with NBD-PS (top) and SITS (bottom) and suspended in either 5 mM phosphate buffer or PBS at 4 °C. The NBD-PS domains behaved similarly to the domains of ghosts double-labeled with NBD-PC and SITS. For example, in the ghosts that were suspended in 5 mM phosphate buffer, most of the band 3 and NBD-PS domains were distributed with areas less than 5% of the total area of the image. The distributions changed to having a large population of domains with areas between 20% and 30% when the ghosts were suspended in PBS.

Importantly, the domain parameters shown for the SITS-labeled band 3, NBD-PC, and NBD-PS images in Figures 2–5 were independent of the second label. For example, when the distributions of domain radiance values for the ghosts double-labeled with SITS and either NBD-PC or NBD-PS (Figures 2 and 3) are compared, it is evident that the SITS domain radiance values fell within the same range for both experiments. Also, ghosts labeled with SITS alone (i.e., no NBD-labeled phospholipid) have a similar distribution of values. Previous experiments showed NBD-PC, NBD-PS, and dansyl-PC enrichment into domains in double-labeling experiments with ghosts in PBS (Rodgers & Glaser, 1991). Quantitation of these domains demonstrated that they had similar values of enrichment of labeled PC and PS as shown here in Figures 2 and 3 (Rodgers & Glaser, 1993). Thus, the domain radiance values were not changed by additional labeling.

*Association of Spectrin Enrichment with Band 3 Domains.* Band 3 is bound to the major cytoskeletal protein spectrin via ankyrin (Bennett, 1985). To investigate the association between the band 3 domains and the cytoskeleton, SITS-labeled ghosts were immunofluorescently labeled using anti-spectrin IgM monoclonal antibodies and a fluorescein-conjugated secondary antibody (Figure 6). The ghosts were suspended in either 5 mM phosphate buffer (Figure 6A) or PBS (Figure 6B) following the immunofluorescence staining. The ghosts in Figure 6C were fixed prior to staining and were suspended in PBS for microscopy. In Figure 6, the SITS images are on the left, and the fluorescein images are on the right. All of the images were collected at 4 °C except the bottom set in Figure 6B, which was collected at 37 °C.

It is evident in Figure 6 that areas of spectrin enrichment occurred, and they correlated with the presence of the band 3 domains. Again, the domains in the band 3 images were larger and more enriched for the ghosts suspended in PBS rather than 5 mM phosphate buffer (Figure 6, panels B and C, versus Figure 6, panel A). The spectrin images of the unfixed ghosts, in both 5 mM phosphate buffer and PBS, had greater domain enrichments than the fixed ghosts in PBS (Figure 6, panels A and B, versus Figure 6, panel C). The large enrichment of spectrin reflects spectrin aggregation due

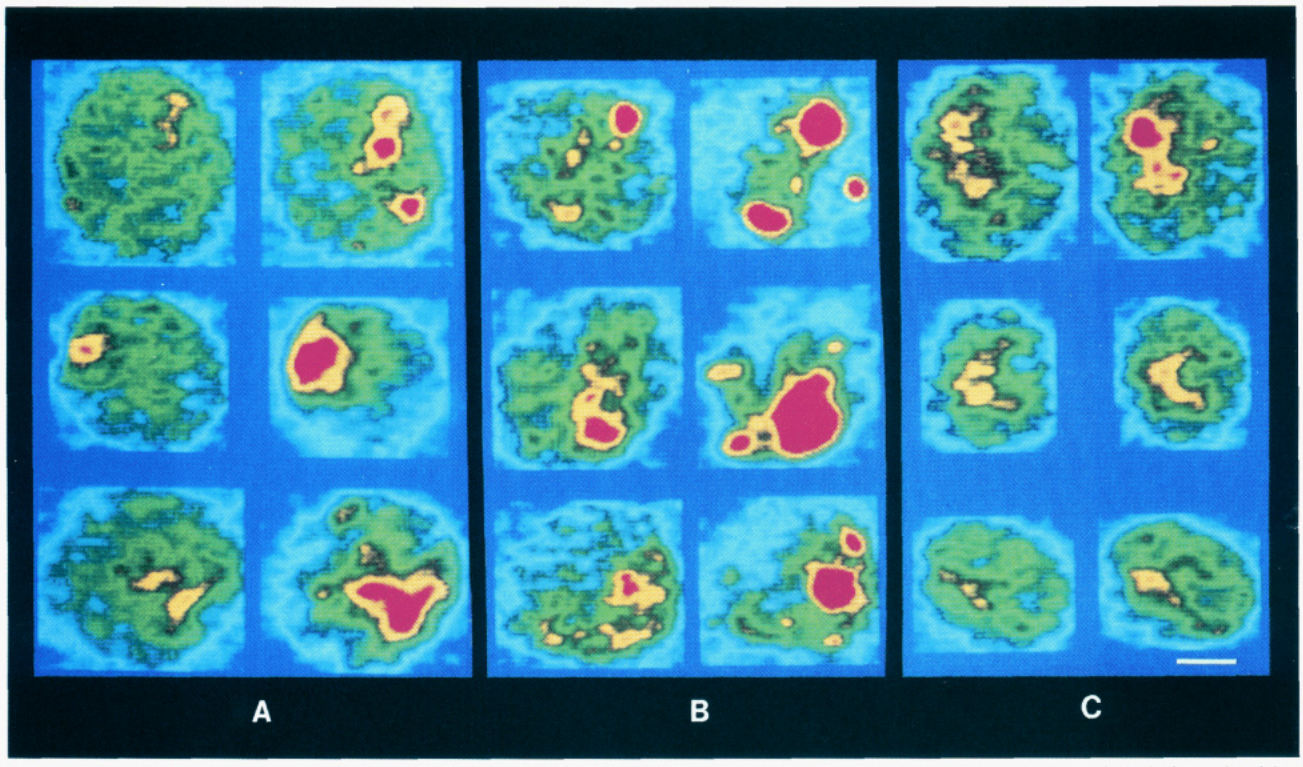


FIGURE 6: Immunofluorescence staining of spectrin and SITS-labeled band 3. Shown here are nine separate double-labeled ghosts in either 5 mM phosphate buffer at 4 °C (A) or PBS at 4 °C (B and C). The ghosts in (C) were suspended in PBS and fixed with glutaraldehyde prior to immunofluorescence staining. The ghosts were labeled with a monoclonal anti-spectrin IgM antibody and with fluorescein-conjugated anti-mouse IgM as the secondary antibody. The SITS images are on the left, and the fluorescein images are on the right. The bottom ghost in (B) was at 37 °C. All images were normalized to a mean gray value of 100 ± 4. The white bar equals 2.5 μm.

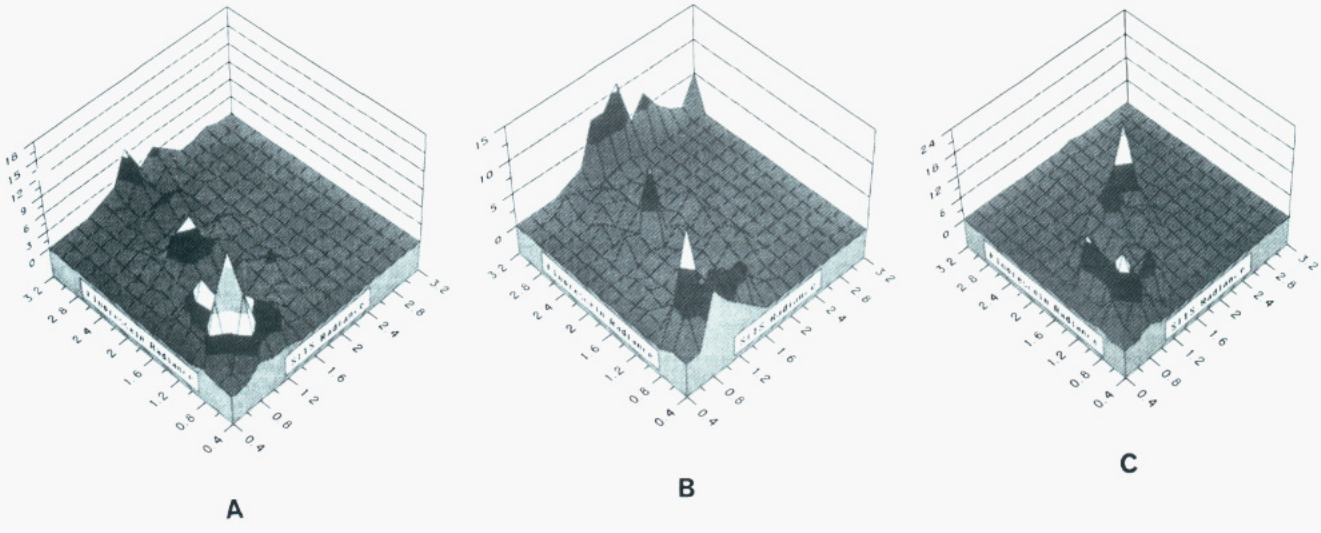


FIGURE 7: Surface plots showing the distributions of domain radiance values for ghosts with SITS-labeled band 3 and fluorescein immunofluorescence staining for spectrin. The surface plots were constructed as described for Figure 2, except that the *x*- and *y*-axes now represent domain enrichment relative to the average radiance of each ghost. The samples were in either 5 mM phosphate buffer at 4 °C (A) or PBS at 4 °C (B and C) as in Figure 6. The distribution in (C) is from ghosts that were fixed in PBS with glutaraldehyde prior to immunofluorescence staining. The sizes of the ghost populations used for the measurements were 40, 42, and 44 for the ghosts in 5 mM phosphate buffer and PBS and the fixed ghosts in PBS, respectively.

to antibody cross-linking. Band 3 enrichment for the ghosts in Figure 6B that were not fixed and suspended in PBS was greater than that of both the fixed ghosts in PBS (Figure 6C) and the ghosts labeled with SITS and NBD-PC only (Figure 1B,C). This demonstrates that aggregation of spectrin resulted in increased enrichment of band 3 in the domains.

Figure 7 shows the distributions of domain radiance values for populations of ghosts corresponding to the conditions in Figure 6. Because of the large enrichment values of the domains in ghosts not fixed before antibody labeling, prenormalized images were used for the measurements. The *x*- and *y*-axes of the plots represent the radiance values of the domains relative to the average radiance of the image. In this manner, a domain radiance of 255 in a ghost normalized to an average radiance of 100 would equal a relative enrichment of 2.55.

Most of the domains represented in Figure 7 for the ghosts that were not fixed were more enriched in fluorescein than SITS. When the distribution of SITS radiance values for the ghosts suspended in PBS (Figures 2B and 7B) are compared, it can be seen that the SITS enrichment was greater when the

anti-spectrin antibody was added. The effect of the anti-spectrin antibody on the SITS enrichment was not observed when the ghosts were maintained in 5 mM phosphate buffer (Figure 7A versus Figure 2A), and this may reflect the weaker binding of band 3 to spectrin at lower ionic strength (Golan & Veatch, 1980; Bennett, 1985).

When the spectrin aggregation was inhibited by fixing the ghosts prior to antibody labeling, the radiance values for the SITS domains resembled the range of values for the ghosts in PBS at 4 °C without antibody labeling (compare Figure 7C to Figure 2B). The distribution of radiance values in Figure 7C occurs along the $x$–$y$ diagonal, representative of domains with similar values of enrichment and depletion for the SITS and fluorescein images.

The concentration range in each ghost was measured using the largest and smallest radiance value in each image. The concentration ranges for the SITS images averaged 2.6, 5.0, and 2.8 for the unfixed ghosts in 5 mM phosphate buffer and PBS and the fixed ghosts in PBS, respectively. The concentration ranges for the fluorescein images averaged 4.9, 17.0, and 3.1 for the unfixed ghosts in 5 mM phosphate buffer and PBS and the fixed ghosts in PBS, respectively. The largest concentration ranges measured for SITS and fluorescein were 13.8 and 75.0, respectively, for unfixed ghosts in PBS.

## DISCUSSION

The abundance of band 3 in the erythrocyte membrane and its close association with spectrin make these proteins good candidates for studying the relationship between protein and lipid distribution. The results showed a correlaton between band 3 domains, spectrin domains, and phosphatidylcholine domains.

The observations described here are consistent with previous work using the fluorescence photobleaching recovery technique on labeled band 3 in erythrocyte ghosts (Golan & Veatch, 1980). For example, Golan and Veatch observed an increase in the immobile fraction of band 3 when ghosts were suspended in high ionic strength buffers rather than low ionic strength buffers. Similarly, the band 3 domains observed here increased in both size and enrichment when the ghosts were suspended in PBS rather that 5 mM phosphate buffer. Therefore, the immobile fraction of band 3 measured by Golan and Veatch probably corresponded to the band 3 domains visualized here.

The correlation between band 3 domains and spectrin domains in immunofluorescently labeled ghosts (Figures 6 and 7) demonstrated an association of the band 3 domains with the cytoskeletal network. The increase in the enrichment and size of the band 3 domains when the ghosts were suspended in PBS rather than 5 mM phosphate buffer is consistent with the cytoskeleton being responsible for forming the band 3 domains. Firmer anchoring of band 3 by the cytoskeleton at higher ionic strengths would reduce band 3 lateral diffusion and act to enrich band 3 in domains. This point is further illustrated by the experiments with spectrin aggregation due to immunofluorescence labeling (Figures 6 and 7). When the immunofluorescently labeled ghosts were suspended in PBS, band 3 enrichment was greater than without antibody labeling. The limited cytoskeleton binding to band 3 in the low ionic strength conditions resulted in only nominal changes in the band 3 distribution induced by spectrin aggregation. It is not clear if the ghosts fixed with glutaraldehyde completely prevented all spectrin aggregation by the antibody labeling. It should be noted also that SITS-labeled band 3 has a different conformation than unlabeled band 3 (Batenjany *et al.*, 1993), and this may in turn affect the ankyrin binding properties of band 3. Thus, the SITS-labeled band 3 studied in the present experiments may represent the distribution of "liganded band 3," which could be different from the unliganded form. Electron microscopy investigations into the erythrocyte cytoskeleton have revealed a heterogeneous structure at the molecular level with dimers, tetramers, and higher order oligomers of spectrin along with associated proteins (Timme, 1981; Liu *et al.*, 1984, 1987; Byers & Branton, 1985; Shen *et al.*, 1986). The distribution of spectrin (fodrin) has been observed to be heterogeneous in many different types of cells and concentrated into domains (Luna & Hitt, 1992). The heterogeneity of spectrin distribution also has been associated with differences in lipid organization (Langner *et al.*, 1992). Thus, changes in the cytoskeleton may represent a mechanism to modulate the surface distribution of band 3 and the organization of lipids in the membrane.

Band 3 is a major component of intramembrane particles seen with freeze–etch electron microscopy. These particles can be induced to aggregate when the spectrin network is distrupted, and studies have shown an association between the distribution of spectrin and the distribution of intramembrane particles (Elgsaeter & Branton, 1974; Elgsaeter *et al.*, 1976; Shotten *et al.*, 1978). Particle aggregation was promoted by increased ionic strength (Elgsaeter & Branton, 1974).

A number of experiments have been done to rule out that the lipid domains in the erythrocyte membrane depend on the fluorophore attached to the phospholipid (Rodgers & Glaser, 1991, 1993). Similar distributions are observed when different fluorophores are attached to the same phospholipid. It is reasonable that, in a fluid membrane, the phospholipid head group may play a more dominant role than the acyl chains in the formation of lipid domains. Attaching the same fluorophore to different head groups changes its distribution in the erythrocyte membrane, and comparing the relative distributions of the different phospholipids appears valid. Also, the distribution of one labeled phospholipid does not depend on the type or concentration of a second labeled phospholipid.

The lack of a pronounced effect of temperature indicates that the lipid domains are not due to a phase transition and the coexistence of gel and liquid-crystalline phase lipids. There were more small NBD-PC domains at 4 than 37 °C in PBS (Figure 4A), and this may reflect the faster lateral mobility observed at higher temperatures (Golan & Veatch, 1980). The faster mobility could manifest itself as smaller domain sizes.

There was a better correlation between band 3 and NBD-PC domains as compared with the band 3 and NBD-PS domains (compare Figure 2 with Figure 3). While many membrane proteins would be expected to influence the distribution of a phospholipid in the membrane, the simplest explanation is that band 3 has a higher binding affinity for phosphatidylcholine than phosphatidylserine and sequesters or enriches phosphatidylcholine in its environment. This may be analogous to the long-range reorganization of phospholipids that can take place with cytochrome $c$ (Haverstick & Glaser, 1989) or with D-$\beta$-hydroxybutyrate dehydrogenase (Wang *et al.*, 1988). Consistent with this suggestion is the observation that there are several phosphatidylcholine molecules that copurify with band 3 (Ross & McConnell, 1978). The tightly bound phospholipids also are enriched in saturated fatty acids (Maneri & Low, 1989). Band 3 was active in reconstituted vesicles composed of phosphatidylcholine and phosphatidylethanolamine, while phosphatidylserine and sphingomyelin inhibited the transport activity (Kohne *et al.*, 1983). The stability of band 3 also was much greater in phosphatidyl-

choline and phosphatidylethanolamine vesicles as opposed to vesicles containing phosphatidylserine and spingomyelin (Maneri & Low, 1988). Since band 3 is a large protein with several transmembrane segments, it can interact with many phospholipids at its surface (Yeagle, 1982), and some experiments suggest a band 3 molecule can perturb approximately 700 phospholipids in a bilayer (Chicken & Sharon, 1984). Because of the large number of band 3 molecules in the red blood cell membrane, it can have a major influence on the distribution of lipids in the membrane.

Membrane protein and lipid domains may represent an important structural motif for membrane function. For example, denatured hemoglobin and a variety of other agents can cause extensive clustering of band 3, which may act *in vivo* as a signal for clearance of aged erythrocytes (Low, 1991). In summary, the results suggest that band 3 plays an important role in forming lipid domains. In turn, the distribution of band 3 is affected by interaction with the cytoskeleton. Since the activity of band 3 and other membrane enzymes is affected by their lipid environment, the lipid domains may be a significant feature in regulating enzyme activity as well as other membrane processes.

## REFERENCES


Batenjany, M. M., Mizukami, H., & Salhany, J. M. (1993) *Biochemistry 32*, 663–668.

Bazzi, M. D., & Nelsestuen, G. L. (1991) *Biochemistry 30*, 7961–7969.

Bennett, V. (1985) *Annu. Rev. Biochem. 54*, 273–304.

Bligh, E. G., & Dyer, W. J. (1959) *Can. J. Biochem. Physiol. 37*, 911–917.

Byers, T. J., & Branton, D. (1985) *Proc. Natl. Acad. Sci. U.S.A. 82*, 6153–6157.

Chicken, C. A., & Sharon, F. J. (1984) *Biochim. Biophys. Acta 774*, 110–118.

Daleke, D. L., & Huestis, W. H. (1985) *Biochemistry 24*, 5406–5416.

Edidin, M., & Stroynowski, I. (1991) *J. Cell Biol. 112*, 1143–1150.

Edidin, M., Kuo, S. C., & Sheetz, M. P. (1991) *Science 29*, 1379–1382.

Elgsaeter, A., & Branton, D. (1974) *J. Cell Biol. 63*, 1018–1030.

Elgsaeter, A., Shotton, D. M., & Branton, D. (1976) *Biochim. Biophys. Acta 426*, 101–122.

Finzi, L., Bustamante, C., Garab, G., & Juang, C.-B. (1989) *Proc. Natl. Acad. Sci. U.S.A. 86*, 8748–8752.

Fowler, V., & Branton, D. (1977) *Nature 268*, 23–26.

Glaser, M. (1993) *Curr. Opin. Struct. Biol. 3*, 475–481.

Golan, V. E., & Veatch, W. (1980) *Proc. Natl. Acad. Sci. U.S.A. 77*, 2537–2541.

Gordan, L. M., & Mobley, P. W. (1984) *J. Membr. Biol. 79*, 75–86.

Haest, C. W. M. (1982) *Biochim. Biophys. Acta 694*, 331–352.

Haverstick, D., & Glaser, M. (1987) *Proc. Natl. Acad. Sci. U.S.A. 84*, 4475–4479.

Haverstick, D. M., & Glaser, M. (1989) *Biophys. J. 55*, 677–682.

Hollenberg, M. D. (1991) *FASEB J. 5*, 178–186.

Jacobson, K., Ishihara, A., & Inman, R. (1987) *Annu. Rev. Physiol. 49*, 163–175.

Jain, M. K. (1983) in *Membrane Fluidity in Biology* (Aloia, R. C., Ed.) Vol. 1, pp 1–37, Academic Press, New York.

Kinnunen, P. K. J. (1991) *Chem. Phys. Lipids 57*, 375–381.

Knauf, P. A., & Rothstein, A. (1971) *J. Gen. Physiol. 58*, 190–203.

Kohne, W., Deuticke, B., & Haest, C. W. M. (1983) *Biochim. Biophys. Acta 730*, 139–150.

Langner, M., Repasky, E. A., & Hui, S.-W. (1992) *FEBS Lett. 305*, 197–202.

Lee, B., McKenna, K., & Bramhall, J. (1985) *Biochim. Biophys. Acta 815*, 128–134.

Liu, S.-C., Windisch, P., Kim, S., & Palek, J. (1984) *Cell 37*, 587–594.

Liu, S.-C., Derick, L. H., & Palek, J. (1987) *J. Cell Biol. 104*, 527–536.

Low, P. S. (1991) in *Red Blood Cell Aging* (Magnani, M., & De Flora, A., Eds.) pp 173–183, Plenum Press, New York.

Luna, E. J., & Hitt, A. L. (1992) *Science 258*, 955–964.

Macara, I. G., & Cantley, L. C. (1983) in *Methods and Reviews* (Elson, E., Frazier, W., & Glaser, L., Eds.) Vol. 1, Plenum Press, New York.

Maneri, L. R., & Low, P. S. (1988) *J. Biol. Chem. 263*, 16170–16178.

Maneri, L. R., & Low, P. S. (1989) *Biochem. Biophys. Res. Commun. 159*, 1012–1019.

Matayoshi, E. D., & Jovin, T. M. (1991) *Biochemisty 30*, 3527–3538.

McClay, D. R., & Ettensohn, C. A. (1987) *Annu. Rev. Cell Biol. 3*, 319–345.

Metcalf, T. N., III, Wang, J. L., & Schindler, M. (1986) *Proc. Natl. Acad. Sci. U.S.A. 83*, 95–99.

Morrow, J. S., Cianci, C. D., Ardito, T., Mann, A. S., & Kashgarian, M. (1989) *J. Cell Biol. 108*, 455–465.

Muhlebach, T., & Cherry, R. J. (1982) *Biochemistry 21*, 4225–4228.

Pessin, J. E., & Glaser, M. (1980) *J. Biol. Chem. 255*, 9044–9050.

Pfeffer, S. R., & Rothman, J. E. (1987) *Annu. Rev. Biochem. 56*, 829–852.

Phillips, W. D., Kopta, C., Blount, P., Gardner, P. D., Steinbach, J. H., & Merlie, J. P. (1991) *Science 251*, 568–570.

Rodgers, W., & Glaser, M. (1991) *Proc. Natl. Acad. Sci. U.S.A. 88*, 1364–1368.

Rodgers, W., & Glaser, M. (1993) in *Optical Microscopy: Emerging Methods and Applications* (Herman, B., & Lemasters, J. J., Eds.) pp 263–283, Academic Press, New York.

Ross, A. H., & McConnell, H. H. (1978) *J. Biol. Chem. 253*, 4777–4782.

Rothberg, K. G., Ying, Y.-S., Kamen, B. A., & Anderson, R. G. W. (1990) *J. Cell Biol. 111*, 2931–2938.

Sheetz, M. P., Schindler, M., & Koppel, D. E. (1980) *Nature 285*, 510–512.

Shen, B. W., Josephs, R., & Steck, T. (1986) *J. Cell Biol. 102*, 997–1006.

Shotton, D., Thompson, K., Wofsy, L., & Branton, D. (1978) *J. Cell Biol. 76*, 512–531.

Shukla, S. D., & Hanahan, D. J. (1982) *J. Biol. Chem. 257*, 2908–2911.

Singer, S. J. (1990) *Annu. Rev. Cell Biol. 6*, 247–296.

Thompson, T. E., & Tillack, T. J. (1985) *Annu. Rev. Biophys. Biophys. Chem. 14*, 361–386.

Timme, A. H. (1981) *J. Ultrastruct. Res. 77*, 199–209.

Tocanne, J.-F., Dupou-Cezanne, L., Lopez, A., & Tournier, J.-F. (1989) *FEBS Lett. 257*, 10–16.

Tsuji, A., Kawasaki, K., Ohnishi, S.-I., Merkle, H., & Kusumi, A. (1988) *Biochemistry 27*, 7447–7452.

Ursitti, J. A., Pumplin, D. W., Wade, J. B., & Bloch, R. J. (1991) *Cell Motil. Cytoskeleton 19*, 227–243.

Wang, S., Martin, E., Cimino, J., Omann, G. M., & Glaser, M. (1988) *Biochemistry 27*, 2033–2039.

Wolf, D. E., Maynard, C. A., McKinnon, C. A., & Melchior, D. L. (1990) *Proc. Natl. Acad. Sci. U.S.A. 87*, 6893–6896.

Yeagle, P. L. (1982) *Biophys. J. 37*, 227–239.

Yechiel, E., & Edidin, M. (1987) *J. Cell Biol. 105*, 755–760.